Analyzing Thermal Efficiency with Pin Fins, Perforated Bases, SolidWorks 2023 Transient Analysis

Serwan S. Talabani†

Department of Manufacturing and Industrial Engineering, Faculty of Engineering, Koya University, Koya, Kurdistan Region – F.R. Iraq

***Abstract* – A group of fifteen central processing unit (CPU) heat sinks of circular, hexagonal, and rectangular shapes with different fin designs and perforation directions was created and analyzed using SolidWorks 2023. In boundary conditions, a heat flux of 65 W was applied, while the surrounding air was at 25°C, and a heat transfer coefficient of 6 W/m²·K was considered. Perforation caused a weight decrease of up to 67.4% in the heat sinks, while perforation orientations had a greater effect on heat dissipation than perforation size. In heat sinks with vertically perforated pins and base R5, the lowest maximum temperature of 77.5°C, the lowest weight of 412.56 g, and the best heat dissipation occurred.**

***Index Terms* – CPU cooling, Heat sink, Perforated base fins, Pin fins, SolidWorks, Transit analysis.**

I. Introduction

Advances in technology, including microelectronics technology, have created a higher demand for cooling solutions that are capable of successfully handling heat generated from such components. It is well known that components in a computer system, such as a CPU, consume a large amount of heat generated through complex calculations. In fact, heat generation in a computer system may affect its performance as well as its longevity in the absence of a cooling system.

Based on recent data, data centers occupy almost 2% of total global power consumption, while at the same time, data centers have experienced steady growth in the previous 2 years. Moreover, it is noted that a substantial part of total power consumption in such systems is ascribed to cooling systems, occupying a range of 30–50%. This is an indication of a challenge in handling high heat flux as well as inhomogeneous heat distribution in electronic components, especially in microchip structures (Huang, et al., 2024).

ARO-The Scientific Journal of Koya University
Vol. XIV, No.2 (2025), Article ID: ARO.12357. 9 pages
DOI: 10.14500/aro.12357
Received: 17 June 2025; Accepted: 23 November 2025
Regular review paper; Published: 29 January 2026
†Corresponding author's e-mail: serwan.talabani@koyauniversity.org

To overcome such challenges, several cooling techniques have been developed, such as cold-water cooling, semiconductor cooling, and liquid nitrogen cooling, although their costs often form an impediment to implementing this technology in practice (Mohan and Govindarajan, 2010). CPU heat sinks represent a convenient and economical cooling technology that relies on principles of heat transfer by conduction, convection, and radiation to get rid of heat from a microprocessor. Examples of heat sinks include flat plates and pin-fin heat sinks. Lower manufacturing cost preferred flat plate models over pin fin structures, but the cooling efficiency of the latter justified their applications in devices for better working conditions (Babus' Haq, Akintunde and Probert, 1995).

The literature exposed the critical role of heat sink designs in improving the cooling process. A simple design manipulation by carving heat sinks into different shapes significantly enhances their heat transfer performance. The verification for such improvement upon perforation introduction is physically well-established and mainly attributed to a larger surface area, which enhances the thermal dissipation efficiency (Damook, et al., 2015; Damook, et al., 2016; Soloveva, Solovev and Shakurova, 2024). The innovative designs of heat sinks beneficially influence the Nusselt number and consistently satisfy the modern devices' requirement for cooling systems.

Simulation programs are powerful tools for engineers to develop eco-efficient structures and designs for different working conditions. These include, but not limited to, simulation of the mechanical stress, heat transfer, and thermal stress under conditions similar to their real-life conditions (Azeez and Mohammed, 2018; Talabani, et al., 2020).

Although previous research has explored perforated fin geometries (Damook, et al., 2015; Al-Muhsen, Al-Khafaji and Ismail, 2023; Kumar, Singh and Verma, 2022; Ismail, Hasan and Ali, 2014; Hussein and Makhoul, 2018), this study is distinct in that it concentrates on a CPU heat sink model subjected to a transient thermal analysis in SolidWorks, as opposed to previous work that mostly focused upon either steady state computational fluid dynamics (CFD) modeling or experimental analysis.

Furthermore, this study also investigates the effects of perforation orientation in relation to heat removal, which encompasses transient analysis results, offering further insights in addition to those of previous research literature into this subject matter topic. Development of a deep understanding regarding the influence of perforation designs and pin shapes on the heat sinks' performance is essential to optimize their cooling efficiency. Therefore, this paper utilized SolidWorks 2023 to simulate the effect of three perforation designs (Circular, Hexagonal, and rectangular) on the transient heat transfer process in the Ryzen 5 2400G CPU running at 65 W. This study aims to quantify how fin geometry and perforation orientation affect transient temperature response under constant heat flux.

II. Design and Modeling of Heat Sinks

SolidWorks is a simulation program characterized by its exceptional capability for mechanical modelling and thermal development analysis (Sam, Arrifin, and Buniyamin, 2012). Fifteen perfectly designed heat sinks were developed using the 2023 version to achieve the goal of this study in understanding the effect of the perforation design on the cooling performance. However, to maintain the compatibility with the design of the CPU, all heat sinks were designed with a square base of dimensions 65 mm × 65 mm. Not to mention, the target of the cooling process is to maintain the processor temperature below 95°C according to the manufacturer's recommendation.

The designs are classified, according to the utilized geometrical shapes, into circular (C), rectangular (R), and hexagonal (H). However, each design has been subdivided into five groups according to their detailed design, which include:

1. Circular-shaped pin fins (C1), Perforated pin and two-sided base (C2), perforated pin and all-sided base (C3), perforated pin only (C4), and vertically perforated pins with a perforated base (C5) were the five models produced within the circular group
2. Hexagonal-shaped pin fins (H1), two-sided perforated base and pins (H2), fully perforated base and pins (H3), perforated fins only (H4), and vertically perforated pins with base (H5) were all part of the hexagonal series
3. Rectangular fins (R1), perforated pin and two-sided base (R2), perforated pin and all-sided base (R3), perforated pin only (R4), and vertically perforated pins with base (R5) were also included in the rectangular designs.

Each model was paired with a standard square silicon heat source (33 mm × 33 mm × 1 mm), replicating the thermal characteristics of a central processing unit to enhance simulation accuracy Fig. 1. The isometric and top views of the fifteen heat sinks.

To maintain uniformity in designs, all models are designed with similar fin heights, perforated areas, as well

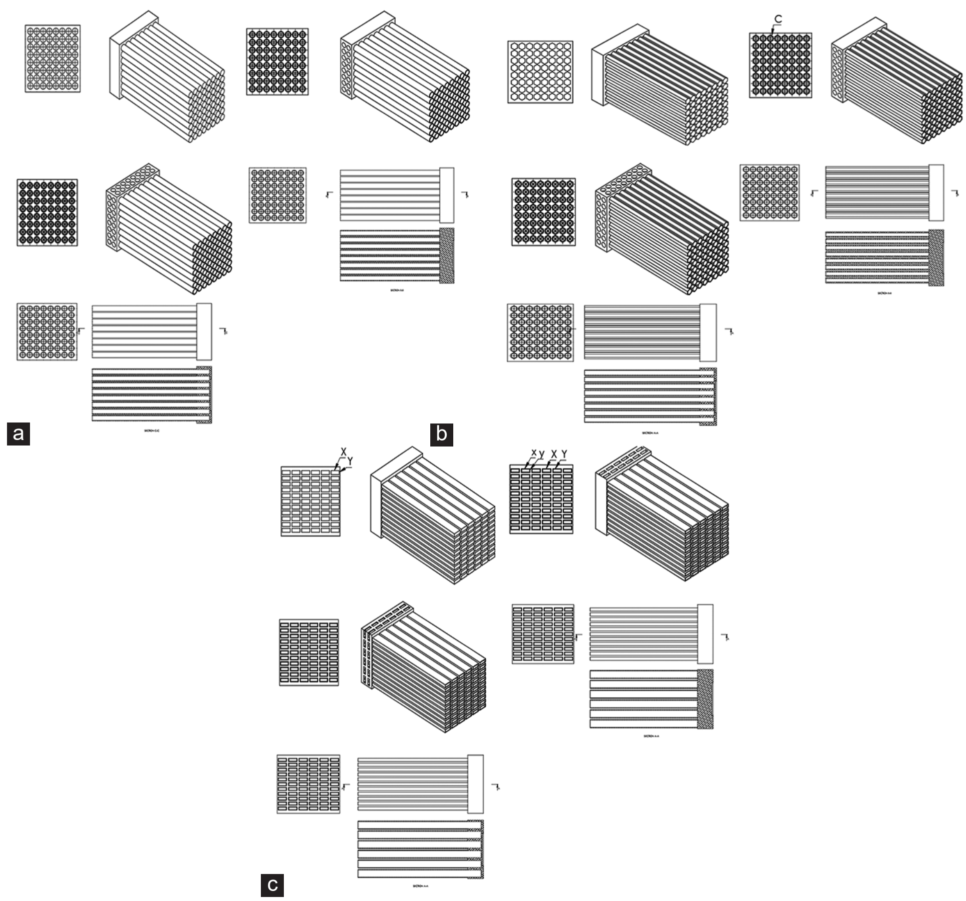

Fig. 1. The fifteen heat sink modules, (a): (C1), (C2), (C3), (C4), (C5). (b): (H1), (H2), (H3), (H4), (H5). (c): (R1), (R2), (R3), (R4), (R5).

as restrictions in terms of spatial constraints suitable for a desktop motherboard package. The base area was designed as 3600 mm^2, with a base height of 15 mm and a fin height of 105 mm. Optimum fin densities have been determined to maximize base area coverage. Variations were introduced in rectangular designs based on geometric constraints. Specific details with respect to designs are provided in Table I.

III. Heat Sink Material Selection

Aluminum alloy was selected as a heat sink material, as it ensures efficient heat transfer, low weight, and cost-effectiveness (Kumar, Singh and Verma, 2022).

IV. Transient Thermal Analysis

The models were tested thermally using the SolidWorks thermal simulation add-in tool. Ambient air temperature and convection heat transfer coefficient were fixed at 25°C (298 K) and 6 W/m·K, respectively. To simulate realistic thermal loading, a 65 W heat source was introduced to represent the operational heat output of the CPU.

A natural convection heat transfer coefficient of h = 6 W/m^2·K was selected, consistent with typical values for air-cooled electronics (2–10 W/m^2·K) (Heat Sink Calculator, n.d.; Incropera and DeWitt, 2002). Previous studies on CPU heat sinks under natural convection reported that the value of convection heat transfer coefficient is between (3 and 7) W/m^2·K, making 6 W/m^2·K a conservative and physically justified choice for this study (Sinson, Kumar and Chennapragada, 2024; Crompton, 2013; Kumar, Singh and Verma, 2022). Under forced convection, values can exceed 10 W/m^2·K and even reach over 50 W/m^2·K depending on airflow conditions (Incropera and DeWitt, 2002), so this assumption provides a reliable baseline for thermal predictions.

The simulation was carried out for a total of 7,200 s, with data collection done at an interval of 360 s. On all exterior surfaces, natural convection was applied as a boundary condition, with the only exceptions being at the points of active heat application. This simulation technique allowed for monitoring of changes in temperatures as well as the thermal performance of different designs.

Heat sink models were imported within the simulation platform for preprocessing and meshing. This aspect was simplified by employing advanced meshing techniques in SolidWorks such that high-resolution analysis was pursued without increasing the processing time. Table II presents a summary of the particular meshes defined for all heat sink designs regarding the discretization of the structure in the entire thermal analysis.

V. Results and Discussion

Figs. 2 and 3 below show the thermal performance of the five circular designs. In C1, where there is no perforation added, the temperature increases steadily to 113.53°C at a total of 7200 s. This is a total temperature change of about 54.36°C.

In the C2 model, after introducing perforations to two sides of both the base and pins, at 360 s, the temperature is 75.48°C. The system reaches a stable condition of 90.18°C at 3240 s, thus recording a lower increment of 14.70°C. Expanding perforations to all sides of the base in the C3 system increases the top surface temperature to 94.52°C at 3240 s, contributing a differential of 13.55°C.

On the contrary, the C4 and C5 designs, with perforations restricted to the pins and vertical perforations in both pins and base, respectively, record a peak temperature of 90.75°C and 88.10°C. Correspondingly, the temperature variation in C4 and C5 designs is recorded as 21.55°C and 16.39°C. This experiment clearly reveals that a higher area of perforations in the base does not lead to a decrease in temperature. Rather, vertical perforations in both pins and base assist in heat dissipation.

As shown in Figs. 4 and 5 below. In configuration H1, without perforations, it is noted that its initial temperature

TABLE I
Dimensions of the Heat Sinks (mm)

Heat sink	Fin's dia.	Fin's side length c	Fin's length x	Fin's width y	No. of fins	No. of perforations	Perforation dia.	Perforation length x	Perforation width y	Horizontal fin's spacing	Vertical fin's spacing	Vertical perforations depth	Horizontal perforations depth
C1	6	-	-	-	64	-	-	-	-	7	7	-	-
C2	6	-	-	-	64	80	5	-	-	7	7	118	65
C3	6	-	-	-	64	96	5	-	-	7	7	118	65
C4	6	-	-	-	64	64	5	-	-	7	7	105	-
C5	6	-	-	-	64	64	5	-	-	7	7	118	-
H1	-	3.3	-	-	64	-	-	-	-	7	7	-	-
H2	-	3.3	-	-	64	80	5	-	-	7	7	118	65
H3	-	3.3	-	-	64	96	5	-	-	7	7	118	65
H4	-	3.3	-	-	64	64	5	-	-	7	7	105	-
H5	-	3.3	-	-	64	64	5	-	-	7	7	118	-
R1	-	-	3.4	8.31	66	-	-	-	-	10	5	-	-
R2	-	-	3.4	8.31	66	78	-	2.616	7.5	10	5	118	65
R3	-	-	3.4	8.31	66	90	-	2.616	7.5	10	5	118	65
R4	-	-	3.4	3.31	66	66	-	2.616	7.5	10	5	105	-
R5	-	-	3.4	8.31	66	66	-	2.616	7.5	10	5	118	-

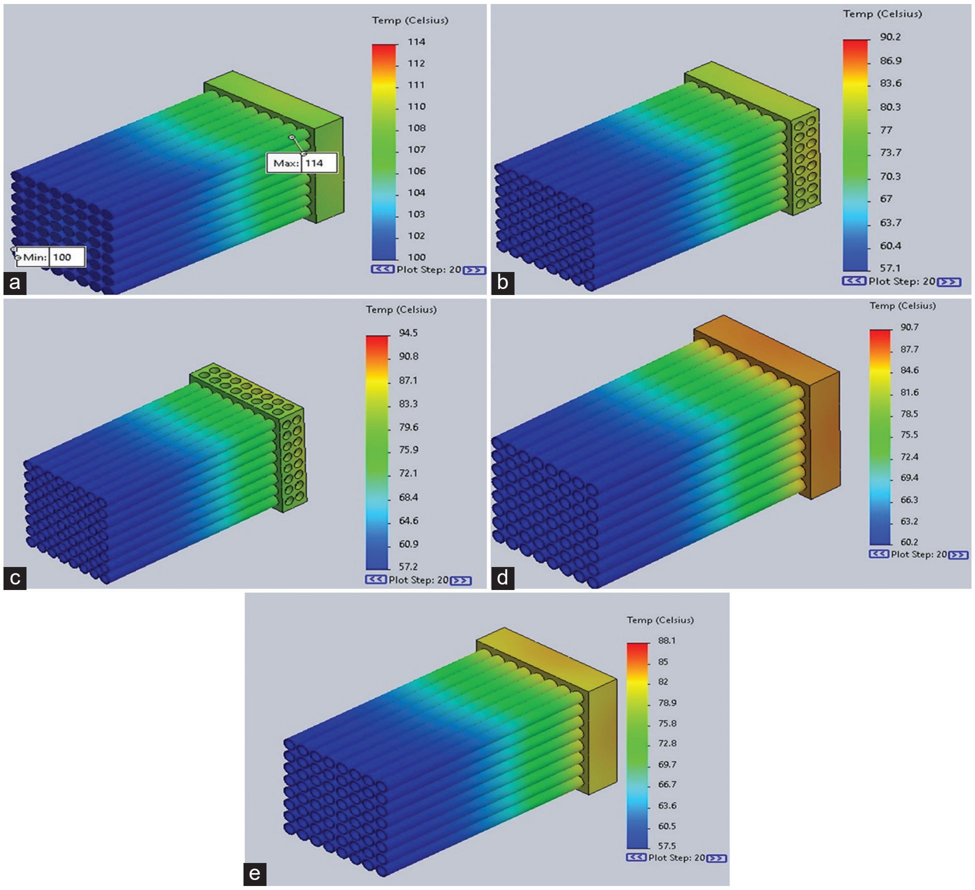

Fig. 2. Temperature distribution of the circular heat sinks (a) C1, (b) C2, (c) C3, (d) C4, and (e) C5.

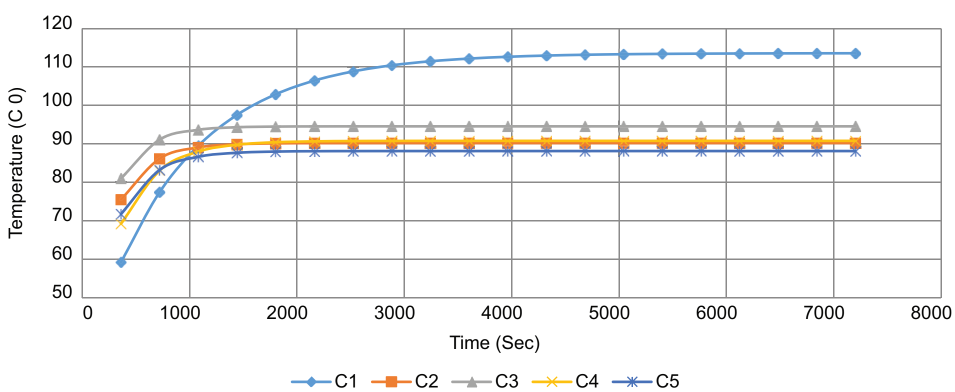

Fig. 3. Graphical representation of transient thermal distribution across various circular heat sinks.

of 58.81°C at a 360-s reading increases to a higher value of 110.08°C at 7200 s. Introducing perforations around two sides of its base in configuration H2 increases its temperature from 74.62 at 360s to a steady value of 88.80°C after 3240 s. Similarly, in configuration H3, where all sides of its base have been provided with perforations, its temperature starts at 80.49°C and attains a steady value of 93.52°C at 7200 s.

On the contrary, it is seen that in the 1st h of the test, both H4 and H5 heat sinks enhance thermal performance. In particular, while H4 configuration reaches an average of around 89.20°C, as soon as it is steady in functionality, in H5, which displays the highest heat dissipation performance in all of them, it is 86.69°C.

Examination of the data for the five rectangular heat sink arrangements illustrated in Figs. 6 and 7 enables a comparison of heat dissipation performance. In the R1 heat dissipation system that lacks perforations, a start temperature of 56.65°C is recorded. During the 7200-s test run, its temperatures continue to climb steadily to a highest recorded value of 96.42°C. This trend suggests that thermal stability in a heating cycle is a challenge for this heat dissipation system.

There is a marked divergence in the behavior of the R2 and R3 designs. In these two designs, perforations are introduced – the perimeter of the base plates of all designs is provided with holes, but in R2, there are holes in two sides, while in R3, all four sides have holes. The initial temperatures of R2

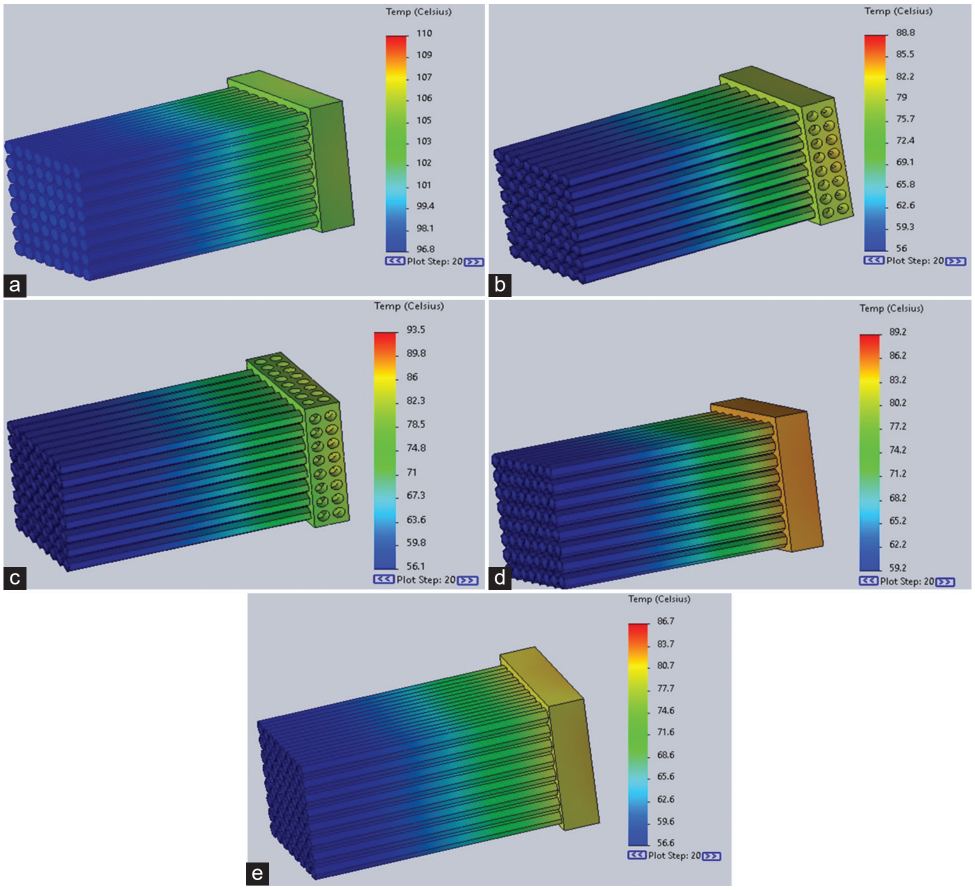

Fig. 4. Temperature distribution of the hexagonal heat sinks (a) H1, (b) H2, (c) H3, (d) H4, (e) H5.

TABLE II
Heat Sinks Meshing Details

Heat sinks	Maximum size of the element (mm)	Minimum size of the element (mm)	Number of elements	Number of nodes
C1	6.8133	2.27100	146838	261171
C2	18.6016	1.91344	205914	406112
C3	18.6070	1.91345	201270	402595
C4	19.8288	1.91343	180934	361395
C5	20.3491	1.91343	210016	408300
H1	6.9615	6.96141	23004	44937
H2	18.8229	1.91344	142773	286256
H3	18.8306	1.91343	137931	282913
H4	20.0816	1.91343	123025	246528
H5	20.5956	1.91343	155886	298424
R1	8.4747	8.47470	9383	21690
R2	11.5950	11.59000	22429	43909
R3	11.5884	11.58830	37433	67454
R4	11.2436	11.24340	17351	34153
R5	11.5480	11.54800	18157	35429

and R3 are higher compared with those of R1 (69.37°C for R2 and 77.67°C for R3), although they attain a stable region sooner than that of R1. At 2880 s, it appears that R2's steady state is 79.49°C, while that of R3 is 87.81°C. This also indicates that too much perforation hinders airflow or leads to a lack of surface contact required for an efficient heat transfer coefficient.

In contrast, a new trend is found in designs R4 and R5, in which vertical perforations are created in either the fins or the fin base. In scheme R4, it starts at 64.55°C and holds steady at 80.22°C at around 3600 s. In scheme R5, it starts at 66.22°C and stabilizes at 77.50°C at 2880 s, making it the most efficient of all the tested designs. This clearly suggests that scheme R5 performs well because vertical perforations in either fin or fin base improve airflow in the fin channel without affecting the points of contact.

In general, it is seen that vertical perforations have a distinct edge over horizontal perforations or a fin without modifications. This particular heat sink configuration registers a lowest recorded temperature of 77.50°C, which is well within the 95°C thermal specs of Ryzen 5 2400G. Its ability to reach thermal equilibrium more quickly than the other configurations suggests strong potential for use in conventional computer cooling systems.

Based on the findings, larger or more extensive perforations do not always yield lower ΔT because of competing effects: (i) Increased convective surface and airflow penetration, (ii) reduced conduction path within fins, and (iii) wake formation and bypass flow diminishing heat transfer. For example, C3 (fully perforated base and pins) performed slightly worse than C4 (pins only), consistent with Huang, Liu and Ay, et al., (2015); Ranjan, Gupta and Bagri,

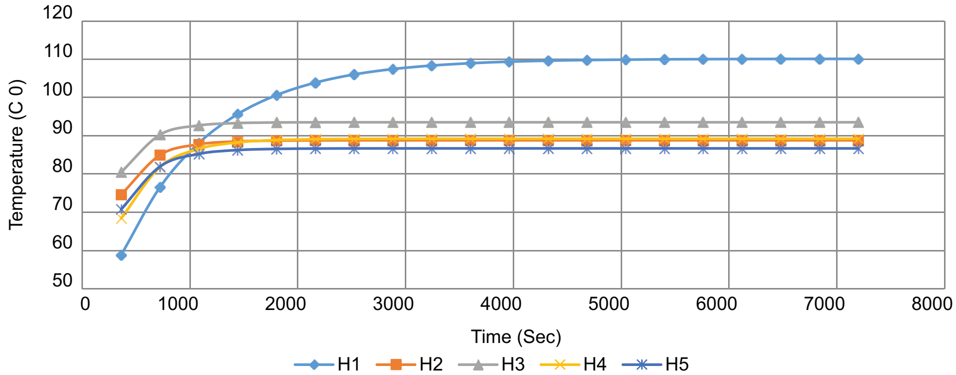

Fig. 5. Graphical representation of transient thermal distribution across various hexagonal heat sinks.

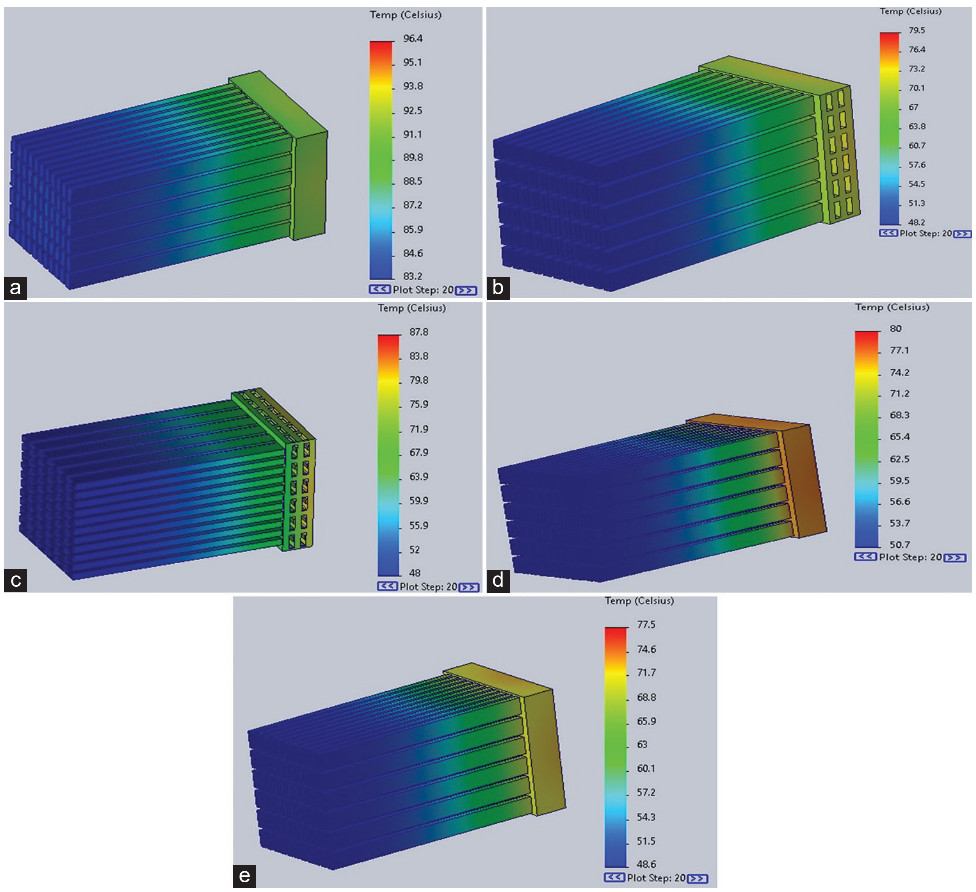

Fig. 6. Temperature distribution of the rectangular heat sinks (a) R1, (b) R2, (c) R3, (d) R4, (e) R5

(2017), who showed optimal perforation exists beyond which conduction reduction offsets convective gains.

By calculating the value of Thermal resistance using thermal resistances (Rth) = (Tmax−Tambient)/Q (Q = 65 W), perforation reduces thermal resistance: C1 ≈ 1.36 K/W → C5 ≈ 0.96 K/W; H1 ≈ 0.81 K/W → H5 ≈ 0.69 K/W; R1 ≈ 0.53 K/W → R5 ≈ 0.49 K/W. These trends are consistent with prior studies reporting Rth reduction with perforated pin-fin arrays under natural or forced convection (Al-Taha, 2018; Luhaibi and Nazzal, 2023).

In terms of the lowest values of ΔT and Rth, rectangular fins (R5) performed better because of increased tip area and uniform airflow passages. Despite perforation, circular and hexagonal fins showed higher values of ΔT, consistent with the findings of Alfian, et al., (2024) regarding the effect of fin cross-section shape on heat transfer performance.

Patterns recorded in terms of temperature differences (ΔT) and Rth match well with those reported in previous studies by Al-Taha, (2018); Luhaibi and Nazzal, (2023); Ranjan, Gupta and Bagri (2017); Huang, Liu and Ay, (2015). Taken together, these findings suggest that the use of perforations leads to an improvement in convective heat transfer rates, although this is possible within a limited

http://dx.doi.org/10.14500/aro.12357

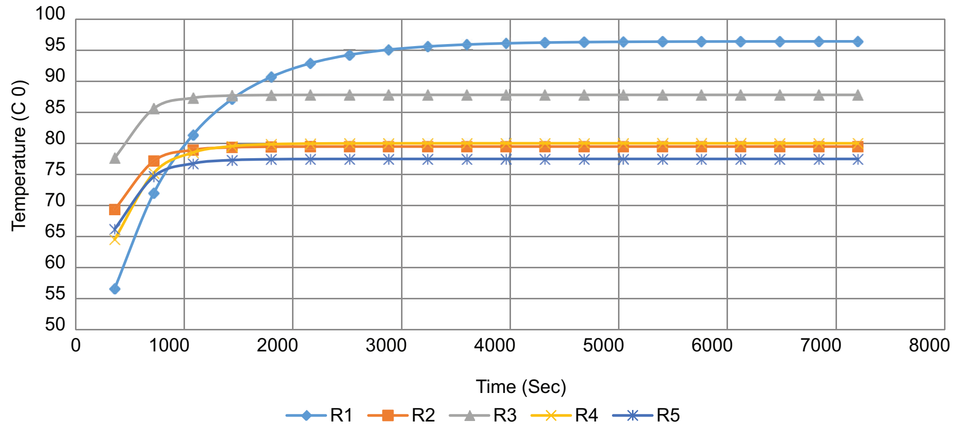

Fig. 7. Graphical representation of transient thermal distribution across various rectangular heat sinks.

extent of perforations. This aspect is well explained in the present study through rectangular perforated fin arrangements (R5).

Table III above highlights that in all cases, because of the integration of perforations in heat-sink designs, a substantial decrease in total weight is achieved. Based on different designs (R, C, and H) considered in this analysis, it is clear that a decrease in total weight ranges from 35% to 67%. In particular, it is noted that designs C3 and H3 have produced a substantial decrease in total weight of 67.29% and 67.40%, respectively. On the contrary, although a decrease of 35.47% was produced in total weight in design R3, a substantial decrease was accomplished nonetheless. This is beneficial in terms of minimizing costs involved in manufacturing as well as increasing overall system efficiency because of lower material usage and component weight.

Each heat sink design (C, H, and R series) was analyzed in SolidWorks using five independent simulations to assess the consistency of the numerical solver and to identify any potential computational variability. The outputs from these repeated simulations were identical for each configuration, indicating a stable solution process and confirming that the solver introduced no measurable numerical uncertainty. Therefore, the standard deviation for multiple simulations of individual geometries was essentially zero. The values of the means and standard deviation in Table IV represent individual differences in five geometries for a set of designs C1 through C5, and individual differences in H1 through H5 and in R1 through R5 designs.

Results have identified that vertically perforated rectangular heat sinks are an excellent technology to be considered in high-performance CPU platforms. Among all designs considered, it has been seen that the performance of configuration R5 is highly effective in maintaining thermal stability at moderate to high processing thermal loads, as shown in Table IV and Fig. 8.

TABLE III
Mass of Heat Sinks with and Without Perforation

Heat sink	Mass before perforation (g)	Mass after perforation (g)	Mass reduction (%)
C1	655.87	–	–
C2	233.24	422.63	64.44
C3	214.51	441.36	67.29
C4	299.61	356.26	54.32
C5	255.5	400.36	61.04
H1	655.59	–	–
H2	232.65	422.94	64.51
H3	213.75	441.84	67.4
H4	299.33	356.26	54.34
H5	255.22	400.36	61.07
R1	671.58	–	–
R2	226.96	444.62	66.2
R3	238.18	433.4	35.47
R4	304.47	367.11	54.66
R5	259.02	412.56	61.43

TABLE IV
Detailed Temperature Differential for All the Heat Sinks

Heat sink	Max. Temp. (°C)	Min. Temp. (°C)	Temp. deference (°C)
C1	113.53	59.168	54.362
C2	90.176	75.481	14.695
C3	94.522	80.972	13.55
C4	90.7	60.2	30.5
C5	88.1	57.5	30.6
(Mean±SD)	95.41±10.39	66.66±10.78	28.74±16.52
H1	110.08	58.814	51.266
H2	88.801	74.624	14.177
H3	93.515	80.493	13.022
H4	89.2	59.2	30
H5	86.7	56.6	30.1
(Mean±SD)	93.66±9.51	65.95±10.85	27.71±15.53
R1	88.801	74.624	14.177
R2	79.494	69.37	10.124
R3	87.812	77.67	10.142
R4	80	50.7	29.3
R5	77.5	48.6	28.9
(Mean±SD)	82.72±5.20	64.19±13.62	18.53±9.79

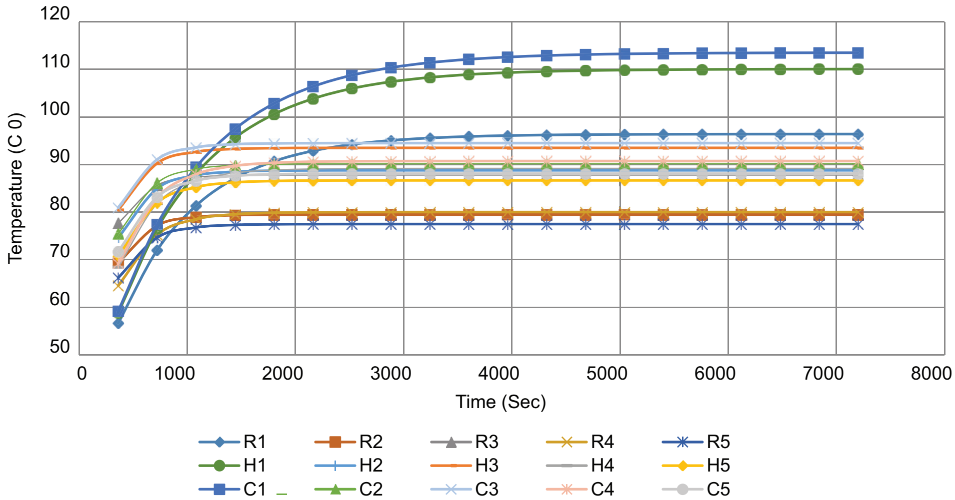

Fig. 8. Graphical representation of transient thermal distribution across various heat sinks.

VI. Conclusion

The fin geometry and orientation of perforations have been explored in this research work for their ability to influence CPU heat sink thermal behavior under a 65 W heating environment, simulated through SolidWorks software version 2023. Based on this simulation, it was observed that some geometries of fins, especially ones that have vertical perforations, have significantly improved convective airflow and heat dissipation performance. These simulation results have been consistent with previous research work carried out by Göksu, (2024) and Damook, et al., (2016).

Of all the tested geometries, the rectangular fin configuration with vertical perforations (R5) had the most stable and efficient thermal behavior, retaining temperatures within a safe operating range and attaining thermal equilibrium extremely quickly. This is consistent with previous studies conducted by Damook, et al., (2016) as well as Alfian, et al., (2024), which have shown and proved the superiority of rectangular perforated fins' ability for efficient heat transfer. Furthermore, this study shows that larger and larger sizes of perforations don't necessarily translate to cooler temperatures, suggesting that orientation, and not sizes, matter more.

One such limitation of the present study can be identified as relating to the meshing operation, and this was simplified by employing advanced meshing techniques available in SolidWorks software. Although this approach allowed for detailed analysis and relatively low computational time, it may potentially lead to slight inaccuracies when compared with more sophisticated or experimentally verified techniques of meshing. To overcome this, future research studies may include experimental verification and a combined or active-passive cooling system as a means of complementing and extending the above numerical analysis provided. In addition, note that this research applies solely on numerical analysis, and though these numerical analyses have been verified through former experimental and CFD studies (Damook, 2016; Alfian et al., 2024), actual experimental.

References

Alfian, D.G.C., Silitonga, D.J., Ramadhan, M.A.F., Ridhwan, I.N., Utomo, R.P., and Rudiarta, I.M., 2024. Comparative analysis of modular pin-fin heat sink performance: Influence of geometric variation on heat transfer characteristics. *International Journal of Integrated Engineering*, 16(6), pp.100-110.

Al-Muhsen, N.F., Al-Khafaji, O.R., and Ismail, F.B., 2023. Thermal performance optimization of perforated fins for flat plate heat sinks using CFD approach. *International Journal of Heat and Technology*, 41(4), pp.1052-1062.

Al-Taha, W.H.A., 2018. Effect of the circular perforations on the heat transfer enhancement by the forced convection from the rectangular fins. *Diyala Journal of Engineering Sciences*, 11, pp.62-70.

Azeez, A., and Mohammed, S.S., 2018. Solidworks simulation of mechanical properties of recycled plastics/nanocomposite faces sandwich panels. *ARO-The Scientific Journal of Koya University*, 6(1), pp.65-70.

Babus' Haq, R.F., Akintunde, K., and Probert, S.D., 1995. Thermal performance of a pin-fin assembly. *International Journal of Heat and Fluid Flow*, 16(1), pp.50-55.

Crompton, J., 2013. *Estimating Heat Transfer Coefficients*. AltaSim Technologies, LLC. Available from: https://altasimtechnologies.com/estimating-heat-transfer-coefficients [Last accessed on 2026 Jan 16].

Damook, A., Kapur, A., Summers, J.L., and Thompson, H.M., 2016. Computational design and optimisation of pin fin heat sinks with rectangular perforations. *Applied Thermal Engineering*, 105, pp.691-703.

Damook, A.A., Kapur, A., Summers, J.L., and Thompson, H.M., 2015. An experimental and computational investigation of thermal air flows through perforated pin heat sinks. *Applied Thermal Engineering,* 89, pp.365-376.

Göksu, T.T., 2024. Investigation of pin and perforated heatsink cooling efficiency and temperature distribution. *Journal of Thermal Analysis and Calorimetry*, 149(12), pp.6517-6529.

Heat Sink Calculator., n.d. *Heat Transfer Coefficients for Natural Convection*. Available from: https://www.heatsinkcalculator.com [Last accessed on 2026 Jan 16].

Huang, C.H., Liu, Y.C., and Ay, H., 2015. The design of optimum perforation diameters for pin fin array for heat transfer enhancement. *International Journal of Heat and Mass Transfer*, 84, pp.752-765.

Huang, H., Zhai, Y., Li, Z., Li, Y., and Wang, H., 2024. Thermal management for microelectronic chips under non-uniform heat flux with supercritical CO_2. *International Journal of Heat and Mass Transfer*, 236, p.126271.

Hussein, M.A., and Makhoul, M.I., 2018. The effect of fins perforation and material type on thermal performance of a heat sink under natural convection. *The Iraqi Journal for Mechanical and Materials Engineering*, 18(3), pp.446-459.

Incropera, F.P., and DeWitt, D.P., 2002. *Fundamentals of Heat and Mass Transfer*. 5th ed. John Wiley and Sons, Hoboken.

Ismail, M.F., Hasan, M.N., and Ali, M., 2014. Numerical simulation of turbulent heat transfer from perforated plate-fin heat sinks. *Heat and Mass Transfer*, 50(4), pp.509-519.

Kumar, A., Singh, A.K., and Verma, A., 2022. Steady state thermal analysis of heat sinks having different types of fins with different types of perforation using ANSYS. *International Journal of Advance Research and Innovative Ideas in Education*, 8(3), pp.5531-5544.

Luhaibi, R.A., and Nazzal, I.T., 2023. Comparison of heat sinks with different perforations number. *NTU Journal of Renewable Energy*, 5(1), pp.93-102.

Mohan, R., and Govindarajan, P., 2010. Thermal analysis of CPU with variable heat sink base plate thickness using CFD. *International Journal of the Computer, the Internet and Management*, 40, pp.27-36.

Ranjan, A., Gupta, V., and Bagri, S., 2017. Effect of perforation shape on the efficiency of heat sink fin - a review. *International Journal for Research Publication and Seminar*, 8(6), pp.1-7.

Sam, R., Arrifin, K., and Buniyamin, N., 2012. Simulation of Pick and Place Robotics System using Solidworks Softmotion. In: *2012 International Conference on System Engineering and Technology (ICSET)*. IEEE, pp.1-6.

Sinson, E., Kumar, R., and Chennapragada, A., 2024. Heat Transfer Coefficient for a Finned CPU Heat Sink under Natural Convection. In: *Paper Presented at the COMSOL Conference 2024*.

Soloveva, O.V., Solovev, S.A., and Shakurova, R.Z., 2024. Numerical study of the thermal and hydraulic characteristics of plate-fin heat sinks. *Processes*, 12(4), p.744.

Talabani, S.S., Azeez, A.T., De Barros, S., Fadhil, B.M., and Omer, H.H., 2020. Effect of modeling techniques on the simulation: Calculating the stress concentration factors in square hollow section T-joints as a case study. *ARO-The Scientific Journal of Koya University*, *8*(1), pp.88-94.